Contribution from the Laboratoire de Synthèse et d'Electrosynthèse Organométallique Associé au CNRS (UA 33), Faculté des Sciences "Gabriel", 21100 Dijon, France, Department of Chemistry, University of Houston, Houston, Texas 77004, Laboratoire de Chimie-Physique Générale, Faculté des Sciences de Rabat, Université Mohammed V, Rabat, Morocco, and Laboratoire de Minéralogie et Cristallographie Associé au CNRS (UA 809), Faculté des Sciences, Centre de 2eme Cycle, 54506 Vandoeuvre-les-Nancy, France

Metalloporphyrins with Metal-Metal Bonds. Synthesis, Characterization, and Electrochemistry of (P)TlMn(CO)$_5$, (P)TlCo(CO)$_4$, and (P)TlM(CO)$_3$Cp Where M = Cr, Mo, and W. Crystal Structure of [(2,3,7,8,12,13,17,18-Octaethylporphinato)thallium(III)]pentacarbonylmanganese

R. Guilard,*[1a] A. Zrineh,[1a,c] M. Ferhat,[1c] A. Tabard,[1a,b] P. Mitaine,[1b] C. Swistak,[1b] P. Richard,[1a] C. Lecomte,[1d] and K. M. Kadish*[1b]

Received July 2, 1987

The synthesis, physicochemical properties, and electrochemistry of a new series of metal-metal σ-bonded thallium porphyrins are reported. The metalate ligands σ-bonded to the thallium octaethyl- or tetraphenylporphyrin complexes were Mn(CO)$_5$, Co(CO)$_4$, W(CO)$_3$Cp, Mo(CO)$_3$Cp, and Cr(CO)$_3$Cp. Each neutral complex was characterized by ^{1}H NMR, IR, and UV-visible spectroscopy, all of which suggested a single metal-metal covalent bond. The crystal structure of (OEP)TlMn(CO)$_5$ was also solved (triclinic, $P\bar{1}$, a = 12.467 (2) Å, b = 13.528 (2) Å, c = 15.088 (3) Å, α = 62.04 (2)°, β = 61.62 (2)°, γ = 69.53 (2)°, Z = 2, $R(F)$ = 0.027, $R_w(F)$ = 0.033, $w = (\sigma^2(I) + 0.04I)^{-1}$). The σ Tl-Mn bond length is 2.649 (1) Å. Electrochemistry and spectroelectrochemistry techniques were used to characterize each oxidized and reduced complex in methylene chloride containing 0.1 M tetrabutylammonium hexafluorophosphate as supporting electrolyte. Each complex underwent two oxidations, which were centered at the porphyrin π ring system. Unlike the case for metal-metal-σ-bonded indium porphyrins, no cleavage of the σ-bond occurs following the first oxidation; i.e., the generated radical cations are stable on the cyclic voltammetry time scale. The metal-metal-bonded compounds could also be reduced by two one-electron additions, but the generated anion radical stability was very low. The ultimate products of electroreduction were the free base porphyrin radical anion and a bis(thallium(I)) compound that was formed from a transient mono(thallium(I)) porphyrin complex.

Introduction

Two classes of bimetallic non-transition-metal porphyrins have been described in the literature.[2] The first includes donor-acceptor complexes of tin and germanium porphyrins that are coordinated to Fe(CO)$_4$, Mn(CO)$_4$HgMn(CO)$_5$, and Co(CO)$_3$-HgCo(CO)$_4$ units.[3-7] The second are the σ-bonded heterobinuclear metalloporphyrins. This class has been limited to indium porphyrins that are coordinated to metalate ions such as Mn(CO)$_5$, Co(CO)$_4$, Cr(CO)$_3$Cp, Mo(CO)$_3$Cp, and W(CO)$_3$Cp.[4,8,9]

Electrochemical studies show that either the nature of the conjugated porphyrin macrocycle or the type of central metal ion in the porphyrin can direct the overall electron transfer mechanism for the specific bimetallic or dimeric transition- or non-transition-metal complex.[6-10] For example, carbenoid porphyrin complexes of (P)SnFe(CO)$_4$ and (P)GeFe(CO)$_4$ are stable after electroreduction[6,7] whereas σ-bonded (P)InM(L) compounds undergo a moderately rapid cleavage of the metal-metal bond after reduction by one or two electrons.[8,9] In contrast to these differences in reductive behavior, both (P)MFe(CO)$_4$ and (P)-InM(L) have similar oxidative behavior that involves a very rapid cleavage of the metal-metal bond after the abstraction of one electron.

Indium-metal and indium-carbon metalloporphyrins show similar physicochemical behavior,[9,11,12] and thus one might expect the electrochemistry of (P)TlM(L) to resemble that of (P)Tl(R), which can be oxidized by one or two electrons without cleavage of the metal-carbon σ-bond.[13] This is indeed the case as shown in the present study of (P)TlM(L), where P = octaethylporphyrin (OEP) and tetraphenylporphyrin (TPP) and M(L) = Cr(CO)$_3$Cp, Mo(CO)$_3$Cp, W(CO)$_3$Cp, Mn(CO)$_5$, and Co(CO)$_4$. Each neutral complex was characterized by IR, UV-visible, and ^{1}H NMR spectroscopy as well as by electrochemistry in nonaqueous media. The singly and doubly oxidized and reduced (P)TlM(L) species were also investigated by UV-visible spectroscopy. The molecular structure of [(2,3,7,8,12,13,17,18-octaethylporphinato)thallium-(III)]pentacarbonylmanganese, (OEP)TlMn(CO)$_5$, was also solved and is described in this paper.

Experimental Section

Chemicals. The synthesis and handling of each bimetallic porphyrin complex and the metalate anions were carried out under an argon atmosphere. All common solvents were thoroughly dried in an appropriate manner and were distilled under argon prior to use. (OEP)TlCl and (TPP)TlCl were obtained by metalation of (OEP)H$_2$ and (TPP)H$_2$ in boiling *N,N*-dimethylformamide.[14] The sodium metalate salts [Cr-(CO)$_3$Cp]Na, [Mo(CO)$_3$Cp]Na, [W(CO)$_3$Cp]Na, [Mn(CO)$_5$]Na, and [Co(CO)$_4$]Na were synthesized according to literature procedures.[15] Reagent grade methylene chloride (CH_2Cl_2, Fisher) and benzonitrile (PhCN, Aldrich) were used for electrochemical studies and were distilled from P_2O_5 prior to use. Tetrabutylammonium hexafluorophosphate ((TBA)PF$_6$) was purchased from Alfa and was recrystallized from ethyl acetate/hexane mixtures prior to use.

General Procedure for Preparation of (P)TlM(L) Where P = OEP and TPP and M(L) = Cr(CO)$_3$Cp, Mo(CO)$_3$Cp, W(CO)$_3$Cp, Mn(CO)$_5$, and Co(CO)$_4$. Table I summarizes percent yields and analytical data for the 10 investigated metal-metal-σ-bonded thallium porphyrins. These

(1) (a) Université de Dijon. (b) University of Houston. (c) Université Mohammed V. (d) Université de Nancy.
(2) Guilard, R.; Lecomte, C.; Kadish, K. M. *Struct. Bonding (Berlin)* **1987**, *64*, 205-268.
(3) Onaka, S.; Kondo, Y.; Toriumi, K.; Ito, T. *Chem. Lett.* **1980**, 1605.
(4) Onaka, S.; Kondo, Y.; Yamashita, M.; Tatematsu, Y.; Kato, Y.; Goto, M.; Ito, T. *Inorg. Chem.* **1985**, *24*, 1070.
(5) Barbe, J.-M.; Guilard, R.; Lecomte, C.; Gerardin, R. *Polyhedron* **1984**, *3*, 889.
(6) Kadish, K. M.; Boisselier-Cocolios, B.; Swistak, C.; Barbe, J.-M.; Guilard, R. *Inorg. Chem.* **1986**, *25*, 121.
(7) Kadish, K. M.; Swistak, C.; Boisselier-Cocolios, B.; Barbe, J.-M.; Guilard, R. *Inorg. Chem.* **1986**, *25*, 4336.
(8) Cocolios, P.; Chang, D.; Vittori, O.; Guilard, R.; Moise, C.; Kadish, K. M. *J. Am. Chem. Soc.* **1984**, *106*, 5724.
(9) Guilard, R.; Mitaine, P.; Moise, C.; Lecomte, C.; Boukhris, A.; Swistak, C.; Tabard, A.; Lacombe, D.; Cornillon, J.-L.; Kadish, K. M. *Inorg. Chem.* **1987**, *26*, 2467.
(10) (a) Collman, J. P.; Prodolliet, J. W.; Leidnmer, C. R. *J. Am. Chem. Soc.* **1986**, *108*, 2916. (b) Brothers, P. J.; Collman, J. P. *Acc. Chem. Res.* **1986**, *19*, 209.
(11) Kadish, K. M.; Boisselier-Cocolios, B.; Cocolios, P.; Guilard, R. *Inorg. Chem.* **1985**, *24*, 2139.
(12) Tabard, A.; Guilard, R.; Kadish, K. M. *Inorg. Chem.* **1986**, *25*, 4277.
(13) Kadish, K. M.; Tabard, A.; Zrineh, A.; Ferhat, M.; Guilard, R. *Inorg. Chem.* **1987**, *26*, 2459.
(14) Buchler, J. W. In *The Porphyrins*; Dolphin, D., Ed.; Academic: New York, 1978; Vol. I, Chapter 10, and references therein.
(15) Piper, T. S.; Wilkinson, G. *J. Inorg. Nucl. Chem.* **1956**, *3*, 104.

0020-1669/88/1327-0697$01.50/0

Table I. Percent Yield and Analytical Data for (P)TlM(L) Complexes

porphyrin, P	metalate anion, M(L)	mol formula	recrystn solvent[a]	yield, %	anal. data[b] % C	% H	% N	% Tl	% M
TPP	$Mn(CO)_5$	$C_{49}H_{28}N_4TlMnO_5$	A/B (2/1)	68	59.0 (58.15)	3.0 (2.79)	5.2 (5.54)	18.8 (20.20)	5.5 (5.43)
	$Co(CO)_4$	$C_{48}H_{28}N_4TlCoO_4$	*c*	63	59.4 (58.35)	3.1 (2.85)	5.5 (5.67)	18.8 (20.68)	4.9 (5.96)
	$Cr(CO)_3Cp$	$C_{52}H_{33}N_4TlCrO_3$	A/B (2/1)	40	59.6 (61.34)	3.5 (3.27)	5.1 (5.50)	16.9 (20.07)	5.0 (5.11)
	$Mo(CO)_3Cp$	$C_{52}H_{33}N_4TlMoO_3$	A/B (2/1)	56	59.0 (58.80)	3.1 (3.13)	5.1 (5.27)	18.7 (19.24)	9.0 (9.03)
	$W(CO)_3Cp$	$C_{52}H_{33}N_4TlWO_3$	A/B (2/1)	55	55.0 (54.30)	2.9 (2.89)	4.8 (4.87)	17.0 (17.77)	15.3 (15.99)
OEP	$Mn(CO)_5$	$C_{41}H_{44}N_4TlMnO_5$	A	83	52.8 (52.83)	4.8 (4.76)	6.1 (6.01)	20.8 (21.92)	5.9 (5.89)
	$Co(CO)_4$	$C_{40}H_{44}N_4TlCoO_4$	*c*	70	52.4 (52.90)	5.2 (4.88)	5.8 (6.17)	22.5 (22.50)	5.1 (6.49)
	$Cr(CO)_3Cp$	$C_{44}H_{49}N_4TlCrO_3$	*c*	46	53.1 (56.33)	5.5 (5.26)	5.3 (5.97)	20.3 (21.78)	5.9 (5.54)
	$Mo(CO)_3Cp$	$C_{44}H_{49}N_4TlMoO_3$	A/B (2/1)	67	53.8 (53.80)	5.0 (5.03)	5.5 (5.70)	20.4 (20.81)	10.1 (9.77)
	$W(CO)_3Cp$	$C_{44}H_{49}N_4TlWO_3$	A/B (2/1)	67	49.8 (49.38)	4.7 (4.62)	5.1 (5.24)	18.3 (19.10)	17.0 (17.18)

[a] Legend: A = benzene; B = heptane. [b] Calculated values in parentheses. [c] Crude compound.

complexes were synthesized by reacting (P)TlCl with $Na^+[ML]^-$ as shown in eq 1. Each metalate ion (0.70 mmol) in tetrahydrofuran (10

$$(P)TlCl + Na^+[M(L)]^- \rightarrow (P)TlM(L) + Na^+ + Cl^- \quad (1)$$

mL) was added dropwise in the dark to (P)TlCl (0.50 mmol) in 130 mL of benzene (or tetrahydrofuran for M(L) = $Cr(CO)_3Cp$). The reaction was monitored by UV–visible spectroscopy and was complete in about 2 h. The solution was evaporated to dryness under vacuum and the residual solid purified in the dark by chromatography over a silica gel packed column under an argon atmosphere (eluant benzene or tetrahydrofuran; column 3 cm × 3 cm; silica gel 70–210 mesh). Evaporation of all the eluant resulted in a crude material, which was recrystallized from benzene/heptane mixtures.

The kinetics for formation of (P)TlM(L) according to eq 1 depend upon the nucleophilic character of the anion.[16] However, the yield of the reaction does not correspond exactly to this parameter (see Table I) but varies according to the nature of $[M(L)]^-$ as shown:

$$[Cr(CO)_3Cp]^- < [Mo(CO)_3Cp]^- \approx [W(CO)_3Cp]^- < [Co(CO)_4]^- < [Mn(CO)_5]^-$$

The resulting $(P)TlCo(CO)_4$ complexes have a very low stability, and all attempts to purify these species were unsuccessful.

Physicochemical Measurements. Elemental analyses were performed by the "Service de Microanalyse" of the CNRS. ^1H NMR spectra at 400 MHz were recorded on a Bruker WM 400 spectrometer of the Cerema ("Centre de Résonance Magnétique de l'Université de Dijon"). Spectra were measured from 5-mg solutions of the complex in C_6D_6 with tetramethylsilane as internal reference. ESR spectra were recorded at 115 K on an IBM Model ER 100 D spectrometer equipped with a Model ER-040-X microwave bridge and a Model ER 080 power supply. The *g* values were measured with respect to diphenylpicrylhydrazyl ($g = 2.0036 \pm 0.0003$). Infrared spectra were obtained on a Perkin-Elmer 580 B apparatus. Samples were prepared as a 1% dispersion in CsI pellets. Electronic absorption spectra were recorded on a Perkin-Elmer 559 spectrophotometer, an IBM Model 9430 spectrophotometer, or a Tracor Northern 1710 holographic optical spectrophotometer–multichannel analyzer.

Cyclic voltammetry measurements were obtained with the use of a three-electrode system. The working electrode was a platinum button, and the counter electrode was a platinum wire. A saturated calomel electrode (SCE) was used as the reference electrode and was separated from the bulk of the solution by a fritted-glass bridge. A BAS 100 electrochemical analyzer connected to a Houston Instrument HIPLOT DMP 40 plotter was used to measure the current–voltage curves.

Controlled-potential electrolysis was performed with an EG&G Model 173 potentiostat or a BAS 100 electrochemical analyzer. Both the reference electrode and the platinum-wire counter electrode were separated from the bulk of the solution by means of a fritted-glass bridge. Thin-layer spectroelectrochemical measurements were performed with an IBM EC 225 voltammetric analyzer coupled with a Tracor Northern 1710 holographic optical spectrophotometer–multichannel analyzer to give time-resolved spectral data. The utilized optically transparent platinum thin-layer electrode (OTTLE) is described in the literature.[17]

Table II. Experimental Conditions

formula	$C_{41}H_{44}N_4TlMnO_5$
fw	932.14
space group	triclinic, $P\bar{1}$
cryst dimens, mm	0.3 × 0.2 × 0.3
cryst color	black
lattice params	
a, *b*, *c*, Å	12.467 (2), 13.528 (2), 15.088 (3)
α, β, γ, deg	62.04 (2), 61.62 (2), 69.53 (2)
V, Å^3; *Z*; ρ_{calcd}, g cm^{-3}	1952; 2; 1.585
μ(Ag Kα), cm^{-1}	24.4
diffractometer	Enraf-Nonius CAD4F (room temp)
radiation	Ag Kα (graphite monochromatized)
scan type; θ_{min}–θ_{max}, deg	ω; 1–21
scan range, deg; scan speed, deg min^{-1}	$1 + 0.45 \tan \theta$; $0.6 < v < 2.0$
aperture, mm	$2 + 5 \tan \theta$
hkl limits	$-15 < h < 15$; $-17 < k < 17$; $0 \le l < 17$
no. of rflns measd	7832
no. of rflns used (*N*)	6317 ($I > 3\sigma(I)$)
no. of params (N_p)	469
N/N_p	13.5
program used	SDP[18]
R(*F*)	0.027
$R_w(F)$	0.033
w	$1/[\sigma^2(I) + 0.04I]$
GOF	1.20

Crystal and Molecular Structure Determination. A suitable crystal of $(OEP)TlMn(CO)_5$ was obtained from recrystallization of the complex in benzene. Preliminary Weissenberg photographs revealed a triclinic cell, isotypic to $(OEP)InMn(CO)_5$.[9] The experimental conditions are given in Table II. The scattering factors were taken from ref 19. A total of 7832 reflections were collected at room temperature, and 6317 ($I > 3\sigma(I)$) were used. The structure was solved by interpretation of the Patterson map and was refined via standard least-squares and Fourier techniques. All non-hydrogen atoms were refined anisotropically whereas hydrogen fractional coordinates were calculated. The final residuals for 469 variables were $R(F) = 0.027$ and $R_w(F) = 0.033$. A summary of the least-squares results is given in Table II. Fractional coordinates of the

(16) Dessy, R. E.; Pohl, R. L.; King, R. B. *J. Am. Chem. Soc.* **1966**, *88*, 5121.

(17) Lin, X. Q.; Kadish, K. M. *Anal. Chem.* **1985**, *57*, 1498.

(18) "SDP: Structure Determination Package"; Enraf-Nonius: Delft, The Netherlands, 1977.

(19) *International Tables for X-Ray Crystallography*; Kynoch: Birmingham, U.K., 1974; Vol. IV.

Table III. Fractional Coordinates, Standard Deviations, and Equivalent Temperature Factors (Å^2) of [(2,3,7,8,12,13,17,18-Octaethylporphinato)thallium(III)]pentacarbonylmanganese

atom	*x*	*y*	*z*	*B*
Tl	0.16230 (1)	0.18340 (1)	0.28635 (1)	2.371 (3)
N(1)	−0.0359 (3)	0.2734 (3)	0.3356 (2)	2.57 (8)
N(2)	0.1084 (3)	0.1852 (2)	0.1620 (2)	2.41 (7)
N(3)	0.2425 (3)	0.0025 (2)	0.2929 (2)	2.56 (8)
O(1)	0.1209 (4)	0.4781 (3)	0.2809 (3)	7.4 (2)
O(2)	0.3403 (4)	0.1991 (4)	0.4245 (3)	6.9 (1)
O(3)	0.5112 (4)	0.1115 (4)	0.1474 (3)	7.0 (1)
O(4)	0.2819 (3)	0.3926 (3)	0.0059 (3)	6.2 (1)
O(5)	0.5245 (3)	0.4482 (4)	0.1093 (4)	8.7 (1)
Mn	0.33272 (5)	0.30934 (5)	0.20500 (4)	3.34 (2)
N(4)	0.0973 (3)	0.0900 (3)	0.4678 (2)	2.58 (8)
C(O1)	0.2017 (5)	0.4132 (4)	0.2530 (4)	4.9 (1)
C(O2)	0.3376 (4)	0.2398 (4)	0.3420 (3)	4.4 (1)
C(O3)	0.4428 (4)	0.1888 (4)	0.1690 (4)	4.5 (1)
C(O4)	0.3015 (4)	0.3612 (4)	0.0812 (4)	4.2 (1)
C(O5)	0.4519 (5)	0.3955 (4)	0.1446 (4)	5.4 (1)
C(1)	−0.0929 (3)	0.3001 (3)	0.4261 (3)	2.67 (9)
C(2)	−0.1888 (3)	0.3981 (3)	0.4111 (3)	3.0 (1)
C(3)	−0.1874 (3)	0.4278 (3)	0.3114 (3)	2.9 (1)
C(4)	−0.0903 (3)	0.3495 (3)	0.2636 (3)	2.73 (9)
C(5)	−0.0571 (3)	0.3489 (3)	0.1619 (3)	2.9 (1)
C(6)	0.0307 (3)	0.2730 (3)	0.1151 (3)	2.72 (9)
C(7)	0.0550 (3)	0.2698 (3)	0.0130 (3)	2.84 (9)
C(8)	0.1503 (3)	0.1840 (3)	−0.0038 (3)	2.9 (1)
C(9)	0.1835 (3)	0.1311 (3)	0.0902 (3)	2.66 (9)
C(10)	0.2729 (3)	0.0355 (3)	0.1104 (3)	2.78 (9)
C(11)	0.2996 (3)	−0.0252 (3)	0.2029 (3)	2.66 (9)
C(12)	0.3888 (3)	−0.1279 (3)	0.2219 (3)	2.9 (1)
C(13)	0.3860 (3)	−0.1573 (3)	0.3223 (3)	3.0 (1)
C(14)	0.2928 (3)	−0.0753 (3)	0.3669 (3)	2.65 (9)
C(15)	0.2575 (3)	−0.0767 (3)	0.4697 (3)	2.8 (1)
C(16)	0.1679 (3)	−0.0015 (3)	0.5168 (3)	2.55 (9)
C(17)	0.1343 (3)	−0.0072 (3)	0.6251 (3)	2.71 (9)
C(18)	0.0445 (3)	0.0819 (3)	0.6387 (3)	2.62 (9)
C(19)	0.0214 (3)	0.1434 (3)	0.5391 (3)	2.56 (9)
C(20)	−0.0652 (3)	0.2401 (3)	0.5185 (3)	2.8 (1)
C(25)	−0.2677 (4)	0.4541 (3)	0.4920 (3)	3.8 (1)
C(26)	−0.2016 (6)	0.5284 (5)	0.4917 (5)	6.5 (2)
C(27)	−0.2746 (4)	0.5175 (4)	0.2608 (3)	4.0 (1)
C(28)	−0.3842 (4)	0.4724 (5)	0.2854 (4)	5.7 (2)
C(29)	−0.0200 (4)	0.3447 (4)	−0.0559 (3)	3.5 (1)
C(30)	−0.1403 (4)	0.3058 (5)	−0.0133 (4)	5.2 (2)
C(31)	0.2097 (4)	0.1430 (4)	−0.0950 (3)	3.7 (1)
C(32)	0.1643 (5)	0.0405 (4)	−0.0712 (4)	5.4 (1)
C(33)	0.4624 (4)	−0.1897 (3)	0.1452 (3)	3.6 (1)
C(34)	0.3885 (5)	−0.2608 (4)	0.1493 (4)	4.7 (1)
C(35)	0.4648 (4)	−0.2510 (4)	0.3798 (3)	3.8 (1)
C(36)	0.5595 (4)	−0.2102 (5)	0.3847 (4)	5.0 (1)
C(37)	0.1944 (4)	−0.0954 (4)	0.7020 (3)	3.6 (1)
C(38)	0.3185 (5)	−0.0745 (5)	0.6774 (4)	5.6 (2)
C(39)	−0.0193 (4)	0.1176 (4)	0.7338 (3)	3.6 (1)
C(40)	0.0287 (5)	0.2159 (4)	0.7166 (4)	5.4 (1)

non-hydrogen atoms are given in Table III. Main bond distances and angles are given in Table IV. Lists of other bond distances and angles, anisotropic thermal parameters, hydrogen coordinates, least-squares planes, and structure factors are given in the supplementary material.

Results and Discussion

Characterization of Neutral (P)TlM(L). Infrared spectroscopic data of the (P)TlM(L) complexes in the solid state are reported in Table V. Only the vibrational frequencies not observed for the starting (P)TlCl derivatives are listed in this table. The ν_{CO} characteristic vibrations of the M(L) ligand appear in the range of 2092–1902 cm^{-1} whereas the ν_{MCO} and ν_{MC} modes have vibrations between 668 and 463 cm^{-1}.[20] For some complexes these last two vibrations are superimposed with those of the porphyrin ring. Vibrations of the perpendicular C–H stretching modes of the cyclopentadienyl substituents occur in the range of 1418–818 cm^{-1} and are only observed for the octaethylporphyrin complexes.[20–23]

Table IV. Bond Distances (Å), Angles (deg) and Standard Deviations in the Coordination Polyhedron and $Mn(CO)_5$ Ligand

Tl–Mn	2.6494 (9)	Mn–C(O4)	1.846 (8)
Tl–N(1)	2.267 (3)	Mn–C(O5)	1.834 (8)
Tl–N(2)	2.255 (6)	O(1)–C(O1)	1.141 (8)
Tl–N(3)	2.267 (4)	O(2)–C(O2)	1.106 (8)
Tl–N(4)	2.265 (3)	O(3)–C(O3)	1.125 (8)
Mn–C(O1)	1.841 (6)	O(4)–C(O4)	1.130 (9)
Mn–C(O2)	1.855 (6)	O(5)–C(O5)	1.12 (2)
Mn–C(O3)	1.845 (6)		
Mn–Tl–N(1)	115.4 (1)	C(O1)–Mn–C(O2)	88.2 (3)
Mn–Tl–N(2)	114.45 (9)	C(O1)–Mn–C(O3)	169.7 (3)
Mn–Tl–N(3)	113.4 (2)	C(O1)–Mn–C(O4)	89.9 (4)
Mn–Tl–N(4)	114.8 (1)	C(O1)–Mn–C(O5)	96.6 (3)
N(1)–Tl–N(2)	79.9 (2)	C(O2)–Mn–C(O3)	90.3 (3)
N(1)–Tl–N(3)	131.3 (2)	C(O2)–Mn–C(O4)	167.6 (3)
N(1)–Tl–N(4)	80.3 (1)	C(O2)–Mn–C(O5)	96.7 (3)
N(2)–Tl–N(3)	80.0 (2)	C(O3)–Mn–C(O4)	89.4 (3)
N(2)–Tl–N(4)	130.8 (2)	C(O3)–Mn–C(O5)	93.8 (3)
N(3)–Tl–N(4)	80.2 (1)	C(O4)–Mn–C(O5)	95.8 (3)
Tl–Mn–C(O1)	84.9 (2)	Mn–C(O1)–O(1)	179.0 (7)
Tl–Mn–C(O2)	84.9 (2)	Mn–C(O2)–O(2)	179.2 (7)
Tl–Mn–C(O3)	84.8 (2)	Mn–C(O3)–O(3)	179.0 (7)
Tl–Mn–C(O4)	82.7 (2)	Mn–C(O4)–O(4)	180 (1)
Tl–Mn–C(O5)	177.9 (2)	Mn–C(O5)–O(5)	178.3 (6)

IR data in the carbonyl region agree with a C_s local symmetry around the axial metal for all of the metal–metal-σ-bonded derivatives and are similar to data for the related bimetallic (P)InM(L) analogues.[9] Consequently, the same assignments can be proposed. In particular, an A″ mode is observed at lower frequencies when a $M(CO)_3Cp$ ligand is coordinated to the thallium porphyrin. There are also two other vibrations associated with A′ modes. These are located in the range of 2092–1912 cm^{-1}.

The effects of the porphyrin macrocycle on the frequency vibrations of (P)InM(L) and (P)TlM(L) are weak, and only small shifts toward high frequencies are noted on going from P = OEP to P = TPP. In contrast, changes in the central metal result in large shifts in vibrations of the M(L) ligand. For example, a ν_{CO} band shift of about 24 cm^{-1} toward lower frequencies is observed between the (P)InM(L)[9] and the (P)TlM(L) complexes and is due to the larger electronegativity of the thallium ion (Tl^{III}, 2.04; In^{III}, 1.78).

UV–visible spectoscopic data of (P)TlM(L) in benzene are summarized in Table VI. Also included in this table are data for the starting materials, (OEP)TlCl and (TPP)TlCl. The electronic absorption spectra of (TPP)Tl$W(CO)_3Cp$ and (TPP)TlCl in benzene are presented in Figure 1. A split Soret band and two or three Q bands are observed for all of the thallium–metal complexes. The Soret band II appears in the range of 443–458 nm depending upon the porphyrin macrocycle and the metalate ligand. This band is slightly red shifted for the TPP compounds and has a larger intensity due to the different donor character of the two macrocycles.[24] The second blue-shifted Soret band (band I) appears in the range of 350–369 nm (see Table VI and Figure 1a) and can be attributed to a $6p_z \rightarrow e_g(\pi^*)$ transition. These electronic absorption spectra belong to the hyper class[2,13,25–27] and provide further evidence for the existence of a σ metal–metal bond in the (P)TlM(L) complexes.

The ratio of the molar absorptivities (ϵ(II)/ϵ(I)) for the split Soret bands I and II of (P)TlM(L) varies from 2.25 for

(20) Nakamoto, K. In *Infrared and Raman Spectra of Inorganic and Coordination Compounds*, 3rd ed.; Wiley: New York, 1978; Part III, and references therein.

(21) Dehand, J.; Pfeffer, M. *J. Organomet. Chem.* **1976**, *104*, 377.
(22) Braunstein, P.; Dehand, J. *Bull. Soc. Chim. Fr.* **1975**, 1997.
(23) King, R. B. *Inorg. Chim. Acta* **1968**, *2*, 454.
(24) Gouterman, M. In *The Porphyrins*; Dolphin, D., Ed.; Academic: New York, 1978; Vol. III, Chapter 1, and references therein.
(25) Cocolios, P.; Guilard, R.; Fournari, P. *J. Organomet. Chem.* **1979**, *179*, 311.
(26) Coutsolelos, A.; Guilard, R. *J. Organomet. Chem.* **1983**, *253*, 273.
(27) Kadish, K. M.; Boisselier-Cocolios, B.; Coutsolelos, A.; Mitaine, P.; Guilard, R. *Inorg. Chem.* **1985**, *24*, 4521.

Table V. Solid-State IR Data of (P)TlM(L) Complexes (CsI Pellets)

porphyrin, P	axial ligand, M(L)	ν_{CO}, cm^{-1}				ν_{MCO} and ν_{MC}, cm^{-1}					$\nu_{(CH)L}$,[a] cm^{-1}		
TPP	$Mn(CO)_5$	2092	2000	1990		660	647	636	467				
	$Co(CO)_4$	2077	2017	1996	1980			543					
	$Cr(CO)_3Cp$	1984	1927	1905		610	554						
	$Mo(CO)_3Cp$	2000	1935	1911		668	583	560	498	463			
	$W(CO)_3Cp$	1996	1925	1902		667	570	549	463				
OEP	$Mn(CO)_5$	2090	1995	1980	1960	662	648	472					
	$Co(CO)_4$	2074	2016	1997	1974		551	543	488				
	$Cr(CO)_3Cp$	1976	1910	1902		650	614	556	518			1353	
	$Mo(CO)_3Cp$	1992	1918	1910		586	563	496	463		1418	1359	818
	$W(CO)_3Cp$	1995	1912	1906		576	555	486	463		1417	1358	825

[a] C–H stretching modes of the cyclopentadienyl substituents.

Table VI. UV–Visible Data of (P)TlCl and (P)TlM(L) Complexes in Benzene (λ, nm; ϵ, M^{-1} cm^{-1})

porphyrin, P	axial ligand	λ_{max} ($10^{-3}\epsilon$) Soret region I	Soret region II	Q band			ϵ(II)/ϵ(I)
TPP	Cl^-		434 (360.5)	520 (2.7)	566 (13.6)	608 (8.5)	
	$Mn(CO)_5$	358 (28.1)	457 (244.8)	548 (2.1)	592 (7.8)	638 (12.5)	8.78
	$Co(CO)_4$	352 (26.2)	452 (291.5)	540 (1.7)	584 (11.9)	626 (13.9)	11.13
	$Cr(CO)_3Cp$	360 (19.2)	458 (199.9)	548 (0.8)	593 (6.1)	649 (10.0)	10.41
	$Mo(CO)_3Cp$	354 (26.4)	458 (269.4)	548 (2.0)	594 (9.2)	640 (15.1)	10.20
	$W(CO)_3Cp$	350 (28.8)	457 (335.9)	549 (2.7)	594 (11.5)	640 (18.2)	11.66
OEP	Cl^-		418 (225.7)	498 (2.1)	545 (11.8)	582 (10.5)	
	$Mn(CO)_5$	369 (44.7)	450 (110.8)		567 (11.9)	599 (2.7)	2.48
	$Co(CO)_4$	366 (27.8)	443 (104.5)		559 (12.6)	594 (5.3)	3.76
	$Cr(CO)_3Cp$	366 (43.4)	450 (97.7)		567 (13.1)	598 (2.8)	2.25
	$Mo(CO)_3Cp$	362 (38.6)	451 (145.8)		568 (15.1)	600 (2.8)	3.78
	$W(CO)_3Cp$	358 (42.3)	449 (160.4)		568 (17.6)	599 (3.8)	3.79

$(OEP)TlCr(CO)_3Cp$ to 11.66 for $(TPP)TlW(CO)_3Cp$. The exact value of the ratio changes as a function of both the porphyrin macrocycle and the axial M(L) ligand and is a reflection of the degree of electron transfer from the thallium ion to the porphyrin macrocycle. The sensitivity of ϵ(II)/ϵ(I) to changes in the porphyrin macrocycle or axial ligand is larger in the (P)InM(L) series than in the (P)TlM(L) series. This may be due to the larger displacement of the thallium ion from the porphyrin mean plane of (P)TlM(L) compared to that of indium in (P)InM(L) (see crystallographic results). Finally, the ratio of molar absorptivities for bands II and I also shows that the electron-donating ability of the metalate anion is weaker in the metal–metal-bonded (P)TlM(L) complex than that of the alkyl or aryl σ-bonded group in (P)Tl(R).[13] This suggests that the bound M(L) group decreases the electron density on both the thallium metal of (P)TlM(L) and the conjugated porphyrin π ring system.

^{1}H NMR Spectroscopy. The ^{1}H NMR data of (P)TlCl and (P)TlM(L) are summarized in Table VII, and the spectra of $(OEP)TlCo(CO)_4$ and $(OEP)TlMo(CO)_3Cp$ are presented in Figure 2. The meso proton resonances of the octaethylporphyrin derivatives appear between 10.36 and 10.42 ppm, and the pyrrole protons of the tetraphenylporphyrin systems give signals close to 9.10 ppm. These chemical shifts are consistent with a Tl(III) ion,[28] and a weak deshielding compared to that in (P)TlCl. The electron density on the porphyrin macrocycle is less for the (P)TlM(L) derivatives than for the (P)TlCl complexes. The same deshielding is also observed for $(P)Tl(CH_3)$.[13] This is consistent with the σ metal–metal bond in (P)TlM(L) as well as with the electron-donating character of the metalate anion (which was already noted in the above discussion of the UV–visible spectra). No significant differences in the (P)TlM(L) NMR spectra are observed as a function of the different metalate axial ligands.

The methylenic and methylic protons of the octaethylporphyrin complexes appear in the ranges of 4.00–4.08 and 1.87–1.89 ppm in C_6D_6, respectively. The multiplet of the methylenic signal results from an ABX_3 system due to a coupling with the methylic protons, the methylenic protons being nonequivalent. This asymmetry results mainly from a displacement of the metal out of the porphyrin plane[29] and is in agreement with penta-

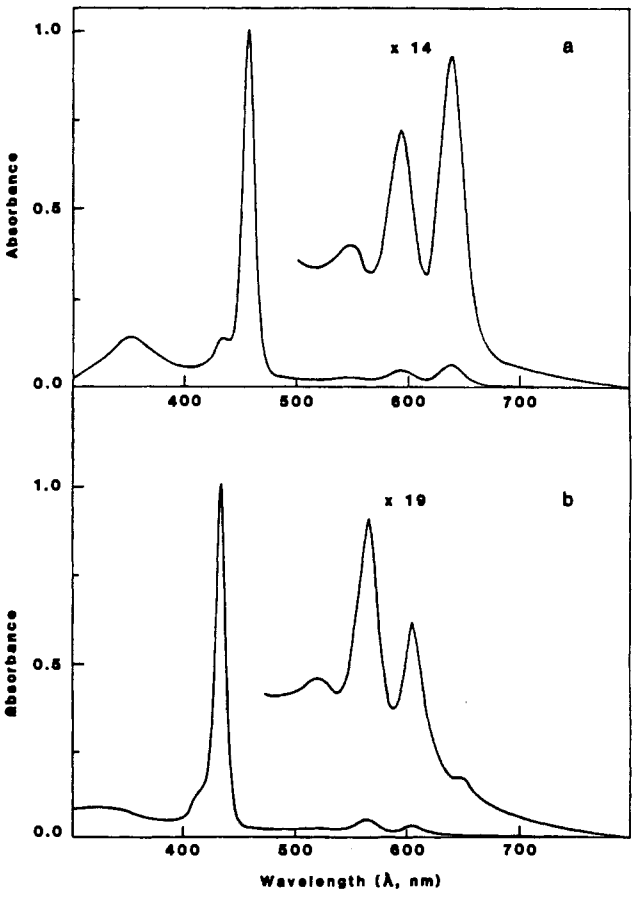

Figure 1. Electronic absorption spectra of (a) $(TPP)TlW(CO)_3Cp$ and (b) (TPP)TlCl in C_6H_6.

(28) Sheer, H.; Katz, J. J. In *Porphyrins and Metalloporphyrins*; Smith, K. M., Ed.; Elsevier: Amsterdam, 1975; Chapter 10.

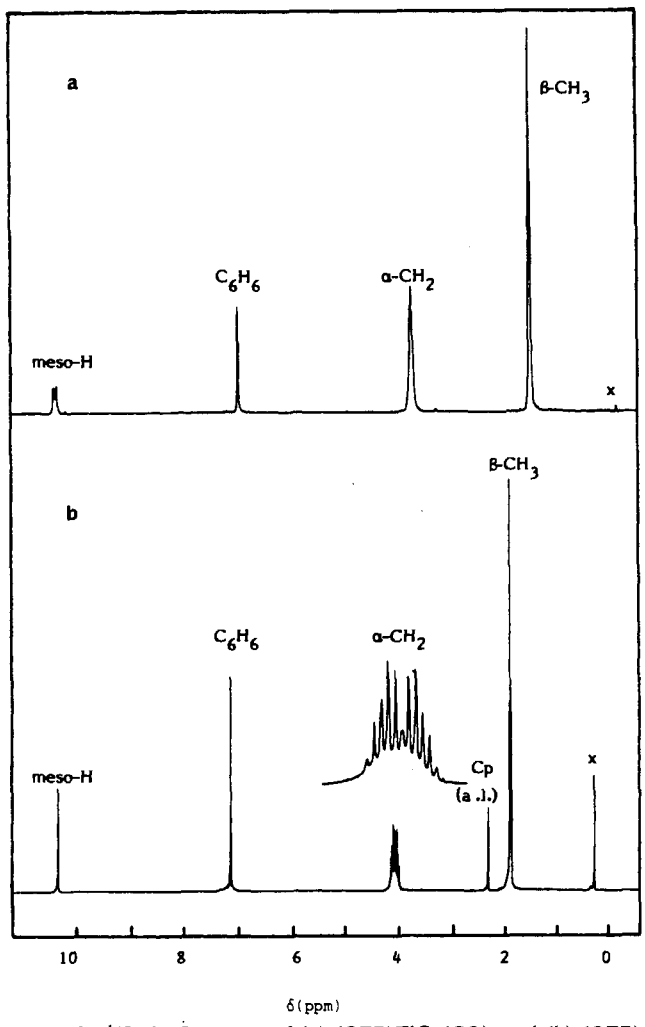

Figure 2. ^{1}H NMR spectra of (a) (OEP)TlCo(CO)$_4$ and (b) (OEP)-TlMo(CO)$_3$Cp recorded at 21 °C in C_6D_6.

coordination of the thallium(III) ion. The inequivalence of the methylenic protons depends on the nature of the axial ligand and increases in the sequence

$$Mn(CO)_5 < Co(CO)_4 < W(CO)_3Cp < Mo(CO)_3Cp < Cr(CO)_3Cp < Cl^-$$

Two factors are responsible for the porphyrin anisotropy. These are the perpendicular metal displacement from the macrocyclic plane and local symmetry of the axial ligand. The NMR data in Table VII unambiguously show that the inequivalence of the porphyrin plane decreases when a metalate ion is coordinated to the thallium metal. The inequivalence is smallest for (P)TlMn-(CO)$_5$ and (P)TlCo(CO)$_4$, which suggests that the local symmetries of the two complexes in solution are probably C_{4v} and C_{3v}, respectively. This same conclusion is reached by analysis of the IR spectroscopy. An anisotropy of the porphyrin plane is also seen in the (TPP)TlM(L) series, and the smallest difference of ortho phenyl proton chemical shift ($|\delta_{o\text{-}H} - \delta_{o'\text{-}H}|$) is observed for the (TPP)TlMn(CO)$_5$ complex (see Table VII).

The axially bound cyclopentadienyl group of (P)TlM(CO)$_3$Cp gives a narrow signal between 1.64 and 2.50 ppm. The shielding of the cyclopentadienyl protons is strong compared to that in other organometallic complexes and is largest for the (OEP)TlCr-(CO)$_3$Cp derivative. This can be explained by the ring current of the porphyrin macrocycle and by the small separation of the cyclopentadienyl protons from the porphyrin. This latter point is confirmed by an X-ray structure of (OEP)InMo(CO)$_3$Cp, which shows the cyclopentadienyl ring tilted toward the macrocycle.[30]

(29) Bushby, C. A.; Dolphin, D. *J. Magn. Reson.* **1976**, *23*, 211.

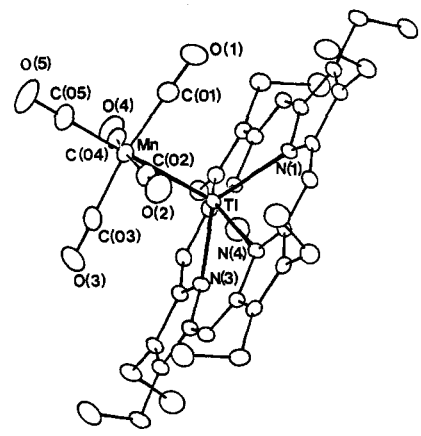

Figure 3. ORTEP drawing and labeling scheme for (OEP)TlMn(CO)$_5$.

The meso and pyrrole protons give a doublet for (OEP)-TlCo(CO)$_4$ and (TPP)TlCo(CO)$_4$. The same spectral morphology is observed for (P)TlCl and results from a coupling between the porphyrin protons and the ^{203,205}Tl metal.[31] This interaction is weaker for the bimetallic (P)TlM(L) derivatives than for the (P)TlCl complexes and also shows that the Co(CO)$_4$ ligand is the only metalate group to possess some electron-withdrawing ability.

Molecular Structure Description. Figure 3 gives an ORTEP view of the (OEP)TlMn(CO)$_5$ complex with the numbering scheme used while Table IV gives the bond distances and bond angles within the coordination polyhedron. (OEP)TlMn(CO)$_5$ is isotypic to (OEP)InMn(CO)$_5$,[9] but the metal–metal-bonding characteristics are slightly different.

It is surprising to note that the metal–metal distance is shorter in (OEP)TlMn(CO)$_5$ than in (OEP)InMn(CO)$_5$ (2.649 (1) vs 2.705 (1) Å). Indeed a different sequence was observed for the metal–axial ligand distances in (TPP)In(CH$_3$) (In–C = 2.132 (15) Å) and (TPP)Tl(CH$_3$) (Tl–C = 2.147 (12) Å) and in (TPP)InCl (In–Cl = 2.369 (2) Å) and (TPP)TlCl (Tl–Cl = 2.420 (4) Å).

As expected, the thallium atom is more out of plane in (OEP)TlMn(CO)$_5$ than the indium atom in (OEP)InMn(CO)$_5$ ($\Delta 4N_{Tl}$ = 0.939 (1) Å, $\Delta 4N_{In}$ = 0.744 (1) Å). The equatorial carbonyl ligands linked to the manganese atom in (OEP)TlMn-(CO)$_5$ are bent toward the porphyrin unit (⟨C–Mn–Tl⟩ = 84.3 (9)°, which is similar to the case for the (OEP)InMn(CO)$_5$ complex. Also these equatorial carbonyl groups do not exactly eclipse the four thallium–nitrogen bonds.

Reduction of (P)TlM(L). Each (P)TlM(L) complex undergoes an irreversible room-temperature reduction in the potential range of CH_2Cl_2. This reduction occurs at E_p values between −1.27 and −1.51 V vs SCE for the (OEP)TlM(L) complexes (see Table VIII). These potentials are similar to $E_{1/2}$ values for the reversible one-electron reduction of several σ-bonded (OEP)Tl(R) derivatives ($E_{1/2}$ = −1.42 to −1.49 V) but negative of E_p = −1.19 V for the irreversible reduction of (OEP)TlCl by cyclic voltammetry in the same solvent/supporting electrolyte system at a scan rate of 0.1 V/s.[13]

The (TPP)TlM(L) complexes have a less basic porphyrin ring than the (OEP)TlM(L) derivatives, and the irreversible reduction of these compounds occurs between −1.11 and −1.30 V vs SCE. Again, this is in the range of potentials for the reversible reduction of several σ-bonded (TPP)Tl(R) complexes ($E_{1/2}$ = −1.17 to −1.27 V) but is negative of E_p = −0.91 V for the irreversible reduction of (TPP)TlCl by cyclic voltammetry in CH_2Cl_2, 0.1 M (TBA)PF_6 at a scan rate of 0.1 V/s.[13]

All of the singly reduced [(P)TlM(L)]$^-$ complexes are characterized by an instability of the metal–metal bond, which is larger than that of the analogous [(P)InM(L)]$^-$ complexes bearing the same axial ligands.[8,9] However, the relative order of stability is reversed for electrooxidation of the metal–metal-bonded complexes.

(30) Guilard, R.; Zrineh, A.; Tabard, A.; Lecomte, C.; Habbou, A.; Richard, P.; Mitaine, P.; Ferhat, M., submitted for publication.

(31) Janson, T. R.; Katz, J. J. In *The Porphyrins*; Dolphin, D., Ed.; Academic: New York, 1978; Vol. IV, Chapter 1.

Table VII. ^{1}H NMR Data[a] for (P)TlCl and (P)TlM(L) Complexes

porphyrin, P	axial ligand	R^1	R^2	protons of R^1			protons of R^2			protons of M(L)[c]	
					mult/*i*	δ		mult/*i*	δ	mult/*i*	δ
TPP	Cl^-	C_6H_5	H	*o*-H	m/8	7.98	pyrr H	d/8	9.03 (63)		
				m-H	m/12	7.42					
				p-H							
	$Mn(CO)_5$	C_6H_5	H	*o*-H	d/4	8.12	pyrr H	s/8	9.09		
				o'-H	d/4	8.33					
				m-H							
				p-H	m/12	7.51					
	$Co(CO)_4$	C_6H_5	H	*o*-H	d/4	8.07	pyrr H	d/8	9.09 (23)		
				o'-H	d/4	8.35					
				m-H							
				p-H	m/12	7.49					
	$Cr(CO)_3Cp$	C_6H_5	H	*o*-H	d/4	8.08	pyrr H	s/8	9.09	s/5	1.86
				o'-H	d/4	8.38					
				m-H							
				p-H	m/12	7.50					
	$Mo(CO)_3Cp$	C_6H_5	H	*o*-H	br/4	8.09	pyrr H	s/8	9.10	s/5	2.50
				o'-H	br/4	8.43					
				m-H							
				p-H	m/12	7.50					
	$W(CO)_3Cp$	C_6H_5	H	*o*-H	br/4	8.09	pyrr H	s/8	9.10	s/5	2.48
				o'-H	br/4	8.44					
				m-H							
				p-H	m/12	7.50					
OEP	Cl^-	H	C_2H_5	meso H	d/4	10.33 (39)[b]	β-CH_3	t/24	1.79		
							α-CH_2	m/8	3.87		
							α'-CH_2	m/8	3.97		
	$Mn(CO)_5$	H	C_2H_5	meso H	s/4	10.36	β-CH_3	t/24	1.89		
							α-CH_2	q/16	4.05		
	$Co(CO)_4$	H	C_2H_5	meso H	d/4	10.42 (22)[b]	β-CH_3	t/24	1.88		
							α-CH_2	m/16	4.02		
	$Cr(CO)_3Cp$	H	C_2H_5	meso H	s/4	10.37	β-CH_3	t/24	1.87	s/5	1.64
							α-CH_2	m/8	4.00		
							α'-CH_2	m/8	4.07		
	$Mo(CO)_3Cp$	H	C_2H_5	meso H	s/4	10.38	β-CH_3	t/24	1.89	s/5	2.32
							α-CH_2	m/8	4.03		
							α'-CH_2	m/8	4.08		
	$W(CO)_3Cp$	H	C_2H_5	meso H	s/4	10.37	β-CH_3	t/24	1.89	s/5	2.30
							α-CH_2	m/8	4.03		
							α'-CH_2	m/8	4.08		

[a] Spectra were recorded in C_6D_6 at 21 °C with $SiMe_4$ as internal reference; chemical shifts downfield from $SiMe_4$ are defined as positive. Legend: R^1 = porphyrin methinic group; R^2 = porphyrin pyrrole group; M(L) = metalate anion; mult = multiplicity; *i* = intensity; s = singlet; d = doublet; q = quartet; m = multiplet; br = broad peak. [b] Values in parentheses are ^1H–$^{203,205}Tl$ coupling constants in Hz. [c] Cyclopentadienyl protons.

This is discussed in the following section of this paper.

Room-temperature cyclic voltammograms show an irreversible reduction for all ten investigated (P)TlM(L) complexes. Eight of the ten metal–metal-bonded species also undergo an irreversible reduction at low temperature, but this is not the case for (TPP)TlMn(CO)$_5$ and (TPP)TlW(CO)$_3$Cp, which exhibit reversible one-electron transfers at low temperature or rapid scan rates. These one-electron reductions occur at −1.22 V for (TPP)TlMn(CO)$_5$ in CH_2Cl_2 at −40 °C and −1.26 V for (TPP)TlW(CO)$_3$Cp at −78 °C. Cyclic voltammograms of these two bimetallic complexes are illustrated in Figure 4.

The generation of $[(P)TlM(L)]^-$ is followed in all cases by an irreversible cleavage of the Tl–M(L) bond. This results in a −30-mV shift of the reduction peak potential, E_p, for each 10-fold increase in potential scan rate and is consistent with the theoretical value predicted for an irreversible chemical reaction that follows a reversible one-electron transfer.[32] The measured values of $|E_{pc} - E_{pc/2}|$ for the reduction of (P)TlM(L) by cyclic voltammetry are approximately 60 mV, and this also indicates an initial reversible one-electron transfer in the first reduction of (P)TlM(L).[32]

The electroreduction mechanism for the (P)TlM(L) complexes parallels that for (P)InM(L)[8,9] in that the initial products of metal–metal bond cleavage are the singly reduced metalloporphyrin and a metalate anion as shown by eq 2. The $[M(L)]^-$ anion cannot be further reduced, but it can be oxidized by one electron to give $[M(L)]_2$ on the reverse potential sweep.[8,9,33-35] The potential for the electrodimerization reaction varies between −0.10 and −0.30 V depending upon the anion and the potential sweep rate and is evident in Figure 4 by well-defined anodic peaks for oxidation of liberated $[Mn(CO)_5]^-$ and $[W(CO)_3Cp]^-$ at 22 °C. These peaks are not present after the reduction of (TPP)TlMn(CO)$_5$ at −40 °C or the reduction of (TPP)TlW(CO)$_3$Cp at −78 °C due to the fact that no cleavage of the metal–metal bond occurs at these temperatures.

$$(P)TlM(L) + e^- \rightleftarrows [(P)TlM(L)]^- \rightarrow (P)Tl^{\bullet} + [M(L)]^- \quad (2)$$

The (P)Tl$^{\bullet}$ species formed by decomposition of $[(P)TlM(L)]^-$ can also undergo a further electroreduction to give $[(P)Tl^I]^-$ in CH_2Cl_2.[13] This species is not stable, and a demetalation occurs, which results in the ultimate formation of both $(P)Tl_2$ and a reduced free base porphyrin. This demetalation is rapid for reduced (P)TlCl[13] and is the most likely factor leading to the high instability of the analogous singly reduced metal–metal-bonded (P)TlM(L) species.

A multielectron transfer is observed for the first reduction of (P)TlM(L) at time scales where decomposition of $[(P)TlM(L)]^-$ occurs. This is evident in Figure 5, which plots the ratio of cathodic

(32) Nicholson, R. S.; Shain, I. *Anal. Chem.* **1964**, *36*, 706.
(33) Lacombe, D. A.; Anderson, J. E.; Kadish, K. M. *Inorg. Chem.* **1986**, *25*, 2074.
(34) Kadish, K. M.; Lacombe, D. A.; Anderson, J. E. *Inorg. Chem.* **1986**, *25*, 2246.
(35) Lemoine, P.; Giraudeau, A.; Gross, M. *J. Chem. Soc., Chem. Commun.* **1980**, 77.

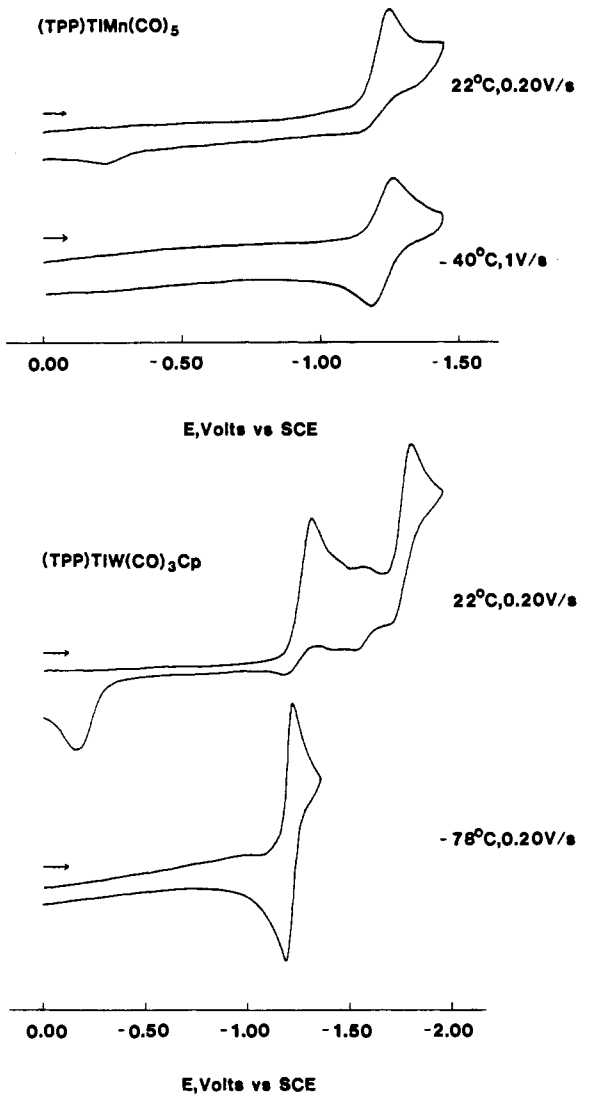

Figure 4. Cyclic voltammograms illustrating the reduction of (TPP)-$TlMn(CO)_5$ and (TPP)$TlW(CO)_3Cp$ at different temperatures and scan rates in CH_2Cl_2, 0.1 M $(TBA)PF_6$.

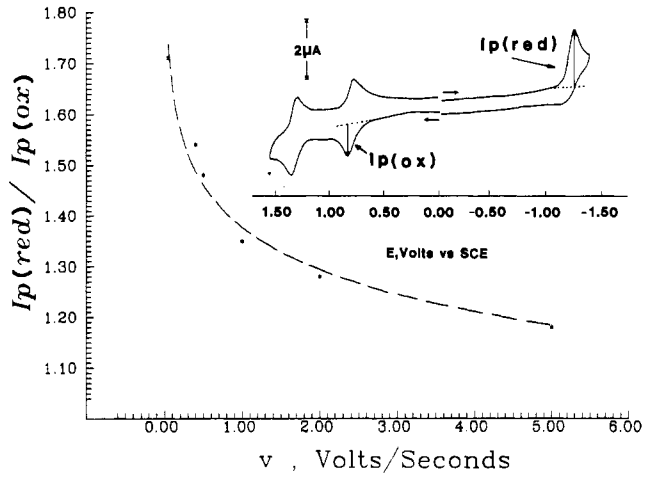

Figure 5. Ratio of peak currents for the first reduction of (TPP)TlMn-$(CO)_5$ and the first oxidation of the same complex in CH_2Cl_2, 0.1 M $(TBA)PF_6$ as a function of scan rate. The insert illustrates a voltammogram of (TPP)$TlMn(CO)_5$ at 0.10 V/s and identifies the measured oxidation and reduction peaks, i_p(ox) and i_p(red).

current for the first reduction of (TPP)$TlMn(CO)_5$ (i_p(red)) to anodic current for the first oxidation of the same species (i_p(ox)) as a function of potential scan rate. The one-electron oxidation of (TPP)$TlMn(CO)_5$ is reversible at room temperature (see Figure 5 insert and following section of the paper) so that the theoretical ratio of $i_p(red)/i_p(ox)$ should be 1.0 if stable $[(TPP)TlMn(CO)_5]^{\bullet-}$ and $[(TPP)TlMn(CO)_5]^{\bullet+}$ radicals are generated by the addition and abstraction of one electron to (TPP)$TlMn(CO)_5$ at negative and positive potentials, respectively.

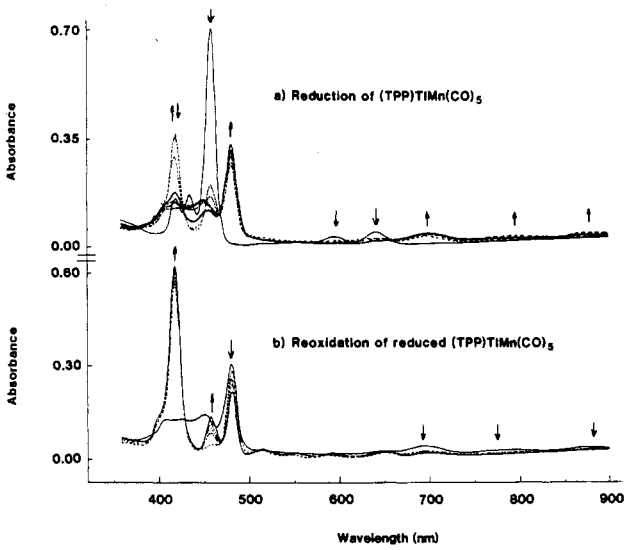

Figure 6. Time-resolved thin-layer spectra during (a) the first reduction of (TPP)$TlMn(CO)_5$ at −1.35 V in CH_2Cl_2, 0.1 M $(TBA)PF_6$ and (b) oxidation of the species in solution at 0.0 V after initial electroreduction.

As seen in Figure 5, a ratio of $i_p(red)/i_p(ox) = 1.0$ is approached at high scan rates. However, the percentage of $[(P)TlMn(CO)_5]^-$ decomposition increases as the scan rate is lowered. (Lower scan rates correspond to longer times before reoxidation of the singly reduced complex.) This results in a larger current for the first reduction and an increased ratio of $i_p(red)/i_p(ox)$. The experimental value of $i_p(red)/i_p(ox)$ is ~1.75 at a scan rate of 0.020 V/s. This corresponds to a situation where the oxidation involves a one-electron transfer while the reduction involves the overall addition of approximately two electrons to the neutral (P)TlM(L) species.

Thin-layer spectroelectrochemistry was used to monitor the electroreduction of (P)TlM(L) and to confirm the above-suggested sequence of steps. Figure 6a illustrates thin-layer spectra recorded during the first reduction of (TPP)$TlMn(CO)_5$. As the reduction proceeds, there is a decrease in the Soret band intensity at 459 nm while bands at 480 and 495 nm increase. The band at 480 nm can be associated with the formation of $(TPP)Tl_2$.[13,36]

Only small amounts of the initial (TPP)$TlMn(CO)_5$ are regenerated after switching the potential back to 0.0 V. This is shown by the spectra of Figure 6b, which are consistent with decomposition of the electrogenerated $[(P)TlM(L)]^-$. The spectrum after oxidation of the initially reduced complex shows a Soret band of $(TPP)Tl_2$ at 480 nm and a Soret band of $(TPP)H_2$ at 419 nm.

The stability of the other $[(P)TlM(L)]^-$ complexes is also low on the thin-layer spectroelectrochemical time scale, and none of the starting spectra could be regenerated after back-electrolysis. In all cases only the final spectra of $(P)Tl_2$ and $(P)H_2$ could be obtained after reduction and oxidation of reduced (P)TlM(L). The instability of $[(P)TlM(L)]^-$ seems to be related to the formation of $(P)Tl^{\bullet}$ after cleavage of the metal–metal bond. The fact that the thallium ion is an electron acceptor and that the LUMO and the metal orbitals are close in energy invariably leads to the formation of a Tl(I) ion after generation of $(P)Tl^{\bullet}$ as a product of $[(P)TlM(L)]^-$ decomposition. The size of the Tl(I) ion (1.47 Å) in reduced $[(P)Tl(I)]^-$ is incompatible with the hole size of the porphyrin core, and a demetalation of these complexes thus occurs.[37-40]

(36) Smith, K. M.; Lai, J.-J. *Tetrahedron Lett.* **1980**, *21*, 433.
(37) Maskasky, J. E.; Kenney, M. E. *J. Am. Chem. Soc.* **1973**, *95*, 1443.

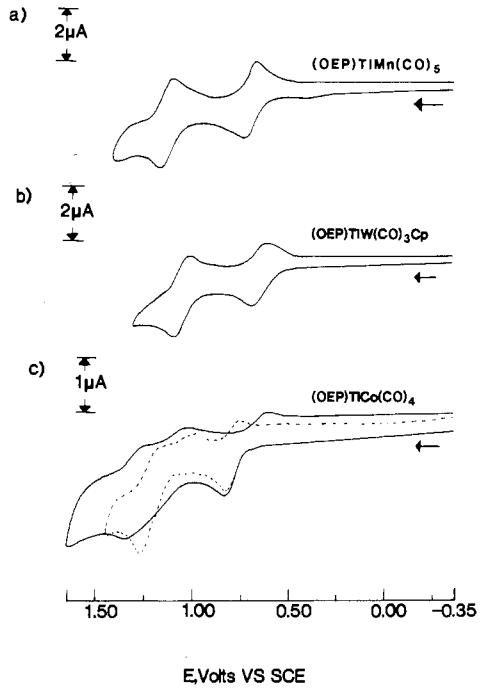

Figure 7. Cyclic voltammograms illustrating the oxidation of (a) $(OEP)TlMn(CO)_5$, (b) $(OEP)TlW(CO)_3Cp$ and (c) $(OEP)TlCo(CO)_4$ at room temperature (—) and at −78 °C (---) in CH_2Cl_2, 0.1 M $(TBA)PF_6$ (scan rate 0.10 V/s).

Table VIII. Half-Wave Potentials ($E_{1/2}$) and Peak Potentials (E_p) for the Oxidation and Reduction of (P)TlM(L) in CH_2Cl_2 Containing 0.1 M $(TBA)PF_6$ at Room Temperature (Scan Rate 0.1 V/s)

porphyrin, P	axial ligand, M(L)	$E_{1/2}$(oxidn)		E_p(redn)
TPP	$Mn(CO)_5$	1.33	0.81	−1.25
	$Co(CO)_4$	1.36[a]	1.01[a]	−1.11
	$W(CO)_3Cp$	1.35	0.76	−1.30
	$Mo(CO)_3Cp$	1.35	0.73	−1.29
	$Cr(CO)_3Cp$	1.36[a]	0.79	−1.15
OEP	$Mn(CO)_5$	1.17	0.74	−1.45
	$Co(CO)_4$		0.85[a]	−1.27
	$W(CO)_3Cp$	1.05	0.65	−1.51
	$Mo(CO)_3Cp$	1.10	0.65	−1.50
	$Cr(CO)_3Cp$		0.71[a]	−1.40

[a] Peak potential, E_p, at a scan rate of 0.10 V/s.

Oxidation of (P)TlM(L). Cyclic voltammograms illustrating the oxidation of $(OEP)TlMn(CO)_5$, $(OEP)TlW(CO)_3Cp$, and $(OEP)TlCo(CO)_4$ in CH_2Cl_2, 0.1 M $(TBA)PF_6$ are shown in Figure 7, and half-wave potentials for electrooxidation of the 10 investigated (P)TlM(L) complexes at 22 °C are summarized in Table VIII. The $(P)TlMn(CO)_5$, $(P)TlW(CO)_3Cp$, and $(P)TlMo(CO)_3Cp$ derivatives undergo reversible electrooxidations which occur at potentials between $E_{1/2}$ = 0.65 and 1.35 V. The $(P)TlCo(CO)_4$ and $(P)TlCr(CO)_3Cp$ complexes are also reversibly oxidized at low temperatures but not at room temperature.

The electrooxidative behavior of (P)TlM(L) differs significantly from that of (P)InM(L), which cannot be reversibly oxidized under any experimental conditions. It is, however, similar to that of (P)Tl(R), which is reversibly oxidized in two steps between $E_{1/2}$ = 0.71 and 1.45 V.[13] The experimentally measured values of $|E_p - E_{p/2}|$ = 64 ± 4 mV and $|E_{pa} - E_{pc}|$ = 60 ± 5 mV for the reversible oxidations of (P)TlM(L) are consistent with a one-electron diffusion-controlled process.[32]

Scheme I

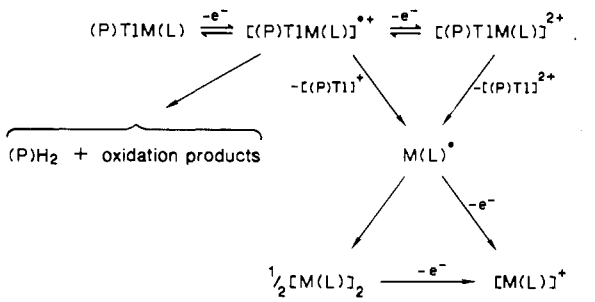

The octaethylporphyrin derivatives show electrochemical behavior similar to that of the tetraphenylporphyrin derivatives but with negatively shifted potentials due to the increased electron-donating properties of the OEP macrocycle. The $[(OEP)TlM(L)]^{\bullet+}$ radical cations are less stable than those of $[(TPP)TlM(L)]^{\bullet+}$, but the specific stability of a given oxidized species is dependent on the nature of the metalate group. The most stable oxidized complexes are $[(TPP)TlMn(CO)_5]^{\bullet+}$, and $[(OEP)TlMn(CO)_5]^{\bullet+}$ while the least stable are $[(OEP)TlCo(CO)_4]^{\bullet+}$ and $[(TPP)TlCo(CO)_4]^{\bullet+}$. The two oxidations of $(OEP)TlCo(CO)_4$ are not well-defined at 22 °C (see solid line, Figure 7c), but the stability of electrogenerated $[(OEP)TlCo(CO)_4]^{\bullet+}$ and $[(OEP)TlCo(CO)_4]^{2+}$ could be increased when the temperature was decreased (dashed line, Figure 7c).

In general, the higher the $\epsilon(II)/\epsilon(I)$ ratio from UV–visible spectra of group 13 metalloporphyrins, the more stable will be the radical cation.[2] Thus, as expected, the $[(P)TlM(L)]^{\bullet+}$ radical cations are much more stable than the $[(P)InM(L)]^{\bullet+}$ derivatives. However, although the (P)TlM(L) derivatives are generally more stable than the indium analogues, the $(P)TlCo(CO_4)$ compounds are still unstable at room temperature. This can be explained by the fact that all of the thallium complexes are easily decomposed by light.

Thin-layer spectra recorded during the one-electron oxidation of $(TPP)TlMn(CO)_5$ confirm the initial formation of a porphyrin π cation radical. The Soret band decreases as the oxidation of $(TPP)TlMn(CO)_5$ proceeds, and new bands characteristic of a porphyrin π cation radical appear at 433 and 732 nm. This oxidation is not totally reversible, and upon back-electrolysis there is a new band at 422 nm and a species with four Q bands. The final spectrum is attributed to $(TPP)H_2$, and this was confirmed by cyclic voltammetry, which, for the case of $(TPP)TlCo(CO)_4$, shows a peak at $E_p \approx 1.3$ V corresponding to reduction of the oxidized free base. The same type of behavior is observed for complexes in the OEP series (see solid line, Figure 7c).

All of the (P)TlM(L) complexes undergo similar electrooxidative behavior. The thin-layer electrolyses were never totally reversible, and the amount of free base formed as a final product varied as a function of the specific porphyrin macrocycle and the metalate anion. As already noted by the cyclic voltammetry experiments, the least stable oxidized complex was $[(OEP)TlCo(CO)_4]^{\bullet+}$.

The electrochemical and spectroscopic data are self-consistent and suggest the overall mechanism given in Scheme I for electrooxidation of (P)TlM(L). Scheme I is similar to one proposed for oxidation of (P)InM(L)[9] but differs with respect to the increased stabilities of the singly and doubly oxidized bimetallic thallium complexes. Decomposition of both $[(P)TlM(L)]^{\bullet+}$ and $[(P)TlM(L)]^{2+}$ leads to M(L)• as one of the major oxidation products. This radical can then dimerize to give $[M(L)]_2$ or be further oxidized to give $[M(L)]^+$ depending upon the scan rate and the temperature. The $[M(L)]_2$ dimer is electrochemically active, and if formed, this species will also be oxidized at potentials positive of 1.0 V vs SCE.[33-35] Under these conditions there will be another oxidation process associated with the overall (P)TlM(L) oxidation. This is illustrated for $(OEP)TlCo(CO)_4$ at room temperature (solid line, Figure 7c) by two overlapping processes, which are associated with the second oxidation.

(38) Abraham, R. J.; Barnett, G. H.; Smith, K. M. *J. Chem. Soc., Perkin Trans. 1* **1973**, 2142.
(39) Giraudeau, A.; Louati, A.; Callot, H. J.; Gross, M. *Inorg. Chem.* **1981**, *20*, 769.
(40) Cullen, D. L.; Meyer, E. F.; Smith, K. M. *Inorg. Chem.* **1977**, *16*, 1179.

In summary, the electronic properties of the thallium ion in (P)TlM(L) lead to several specific properties of these bimetallic metal-metal-bonded complexes. Structural parameters show that the thallium metal ion is significantly more out of the porphyrin plane in (P)TlM(L) ($\Delta 4N$ = 0.939 (1) Å) than the indium metal ion in (P)InM(L)[9] ($\Delta 4N$ = 0.744 (1) Å), and this can explain the symmetry changes of the axial ligand noted by IR spectroscopy. The main differences between complexes in the (P)TlM(L) and the (P)InM(L) series are probably in the larger orbital overlap that occurs between the thallium atom and the axial metal. This results in a shorter metal-metal bond length and a greater stability of both the neutral and the singly or doubly oxidized (P)TlM(L) complexes. For the case of (P)TlMn(CO)$_5$ and (P)TlW(CO)$_3$Cp, this leads to well-defined reversible one- and two-electron oxidations.

Acknowledgment. The support of the CNRS, the National Science Foundation (Grant No. CHD-8515411 and No. INT-8413696), and the Robert A. Welch Foundation (Grant No. E-680) is gratefully acknowledged.

Registry No. (TPP)TlMn(CO)$_5$, 112022-35-2; (TPP)Co(CO)$_4$, 112022-36-3; (TPP)TlCr(CO)$_3$Cp, 112022-37-4; (TPP)TlMo(CO)$_3$Cp, 112022-38-5; (TPP)TlW(CO)$_3$Cp, 112022-39-6; (OEP)TlMn(CO)$_5$, 112041-61-9; (OEP)TlCo(CO)$_4$, 112041-62-0; (OEP)TlCr(CO)$_3$Cp, 112022-40-9; (OEP)TlMo(CO)$_3$Cp, 112022-41-0; (OEP)TlW(CO)$_3$Cp, 112041-63-1; (OEP)TlCl, 58167-68-3; (TPP)TlCl, 63848-51-1; [Cr(CO)$_3$Cp]Na, 12203-12-2; [Mo(CO)$_3$Cp]Na, 12107-35-6; [W(CO)$_3$Cp]Na, 12107-36-7; [Mn(CO)$_5$]Na, 13859-41-1; [Co(CO)$_4$]Na, 14878-28-5.

Supplementary Material Available: Tables of bond distances in angstroms, general displacement parameter expressions (B's), bond angles in degrees, and positional parameters and their estimated standard deviations (11 pages); a table of observed and calculated structure factors (36 pages). Ordering information is given on any current masthead page.

Contribution from the Department of Chemistry, Thimann Laboratories, University of California, Santa Cruz, California 95064, and Drug Dynamics Institute, College of Pharmacy, University of Texas, Austin, Texas 78712

Synthetic Analogue Approach to Metallobleomycins. 3. Synthesis, Crystal and Solution Structures, and Redox Properties of Bis(*N*-(2-(4-imidazolyl)ethyl)pyridine-2-carboxamido)cobalt(III) Perchlorate Hydrate

Karoline Delany, Satish K. Arora,† and Pradip K. Mascharak*

Received August 20, 1987

The cobalt(III) complex of PypepH (**1**), a peptide ligand resembling part of the metal-chelating portion of the antitumor drugs bleomycins (BLM), has been synthesized via aerobic oxidation of a mixture of **1** and cobalt(II) acetate (ratio 2:1) in aqueous or anhydrous methanol. [Co(Pypep)$_2$]ClO$_4$·H$_2$O (**2**) crystallizes in the trigonal space group $P3_121$ with a = 13.434 (3) Å, b = 13.434 (4) Å, c = 11.453 (3) Å, γ = 120.0°, and Z = 3. The structure was refined to R = 5.9% by using 2661 unique data ($F_o^2 > 2.5\sigma(F_o^2)$). The coordination geometry around low-spin Co(III) is octahedral with Co-N(pyridine) = 1.937 (5) Å, Co-N(imidazole) = 1.952 (5) Å, and Co-N(amido) = 1.933 (3) Å, respectively. Electrochemical reduction of **2** in DMF or methanol gives rise to an unstable Co(II) species that is rapidly converted into a high-spin octahedral Co(II) complex. The solution structure of [Co(Pypep)$_2$]$^+$ has been explored with the aid of one- and two-dimensional ^{1}H and ^{13}C NMR spectroscopy.

Introduction

Bleomycins (BLM), a family of glycopeptide antibiotics, induce extensive DNA damage in presence of metal ions like Fe^{2+} and molecular oxygen.[1-6] Clinical use of BLM in treatment of selected neoplastic diseases[6,7] is dependent on the DNA degradation reaction. Since cobalt(II) was reported to inactivate BLM,[8] initial interest in cobalt-bleomycin chelates (Co-BLMs) had been limited to some extent. Nevertheless, the coordination chemistry of Co-BLMs has been explored,[1-6,9-15] and Co-BLMs have found use in specific clinical applications. Co(III)-BLMs exhibit the unusual property of accumulating selectively in the nuclei of certain types of cancer cells, and radiolabeled kinetically inert ^{57}Co(III)-BLMs are used as diagnostic agents in nuclear medicine.[14] Recently, it has been reported that Co(III)-BLM can cause DNA strand breaks when irradiated with UV or visible light.[16-18] In both cases, cleavage of DNA is believed to be a consequence of photoreduction of Co(III)-BLM. This recently discovered bioactivity of Co(III)-BLM, namely, the photoinduced DNA damage by the metallodrug, has prompted renewed interest in the chemistry of Co-BLMs. As part of our "synthetic analogue approach"[19] to metallobleomycins (M-BLMs), we have underaken the task of looking into the structure of a few synthetic analogues of Co-BLMs. Previously we have reported the structures and spectral properties of Cu(II) complexes of two peptides resembling part of the metal-chelating region of BLM.[20] The low-spin Fe(III) complex of one of the peptides, *N*-(2-(4-imidazolyl)ethyl)-pyridine-2-carboxamide (**1**), has also been reported by us.[21] In

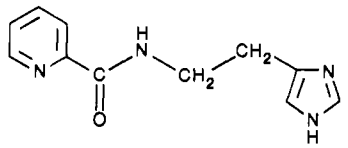

PypepH (1)

* To whom correspondence should be addressed at the University of California.
† To whom inquiries related to crystallographic data should be addressed at the University of Texas.

(1) Sugiura, Y.; Takita, T.; Umezawa, H. *Met. Ions Biol. Syst.* **1985**, *19*, 81.
(2) (a) Dabrowiak, J. C. *Adv. Inorg. Biochem.* **1983**, *4*, 69. (b) Dabrowiak, J. C. *Met. Ions Biol. Syst.* **1980**, *11*, 305. (c) Dabrowiak, J. C. *J. Inorg. Biochem.* **1980**, *13*, 317.
(3) Povrick, L. F. In *Molecular Aspects of Anticancer Drug Action*; Neidle, S., Waring, M. J., Eds.; Macmillan: London, 1983; p 157.
(4) Umezawa, H.; Takita, T. *Struct. Bonding (Berlin)* **1980**, *40*, 73.
(5) *Bleomycin: Chemical, Biochemical and Biological Aspects*; Hecht, S. M., Ed.; Springer-Verlag: New York, 1979.
(6) *Bleomycin: Current Status and New Developments*; Carter, S. K., Crooke, S. T., Umezawa, H., Eds.; Academic: New York, 1978.
(7) Blum, R. H.; Carter, S. K.; Agre, K. A. *Cancer (Philadelphia)* **1973**, *31*, 903.
(8) (a) Sausville, E. A.; Peisach, J.; Horwitz, S. B. *Biochemistry* **1978**, *17*, 2740. (b) Nagai, K.; Suzuki, H.; Tanaka, N.; Umezawa, H. *J. Antibiot.* **1969**, *22*, 569. (c) Nagai, K.; Yamaki, H.; Suzuki, H.; Tanaka, N.; Umezawa, H. *Biochim. Biophys. Acta* **1969**, *179*, 165.
(9) (a) Sugiura, Y. *J. Antibiot.* **1978**, *31*, 1206. (b) Sugiura, Y. *Biochem. Biophys. Res. Commun.* **1979**, *88*, 913. (c) Sugiura, Y. *J. Am. Chem. Soc.* **1980**, *102*, 5216.
(10) (a) Tsukayama, M.; Randall, C. R.; Santillo, F. S.; Dabrowiak, J. C. *J. Am. Chem. Soc.* **1981**, *103*, 458. (b) Dabrowiak, J. C.; Tsukayama, M. *J. Am. Chem. Soc.* **1981**, *103*, 7543.

0020-1669/88/1327-0705$01.50/0